Performance Testing of Micro Loop Heat Pipes

Chin-Chun Hsu, Shung-Wen Kang* and Tung-Fu Hou

Department of Mechanical and Electro-Mechanical Engineering, Tamkang University
Tamsui, Taiwan 251, R.O.C.

Abstract

A 60 mm × 33 mm × 0.8 mm micro loop heat pipe (MLHP), consisting of an evaporator, vapor line, condenser and two liquid lines, was fabricated and characterized. The wicking structure consists of parallel V-grooves with a hydraulic diameter of 47 μm, 67 μm and 83 μm, and is formed by bulk silicon etching. The MLHP was realized by bonding a glass wafer onto a silicon substrate, so as to result in a transparent cover for two-phase flow visualization. Water and methanol were used as the working fluids. The test results showed that water demonstrates a wider heat load performance range (3.3 W~12.96 W) than methanol (1.2 W~5.85 W) for the MLHP with an evaporator area of 1 cm^2 and condenser temperature of 17 °C. The best thermal resistance of the MLHP was 0.106 °C/W, 64 times higher than that without fluid filling. The smaller diameter grooves caused the higher liquid capillarity and enhanced transfer capacity. It was observed that the presence of non-condensable gas negatively affected the reliability of the MLHP and significantly reduced the performance.

***Key Words*:** Micro Loop Heat Pipes, Two Phase Flow, Non-condensable Gas, Thermal Resistance

1. Introduction

The loop heat pipe (LHP) was first presented by Yu. F. Maidanik jointly with his colleagues in the former Soviet Union in the 1980s. The LHP features more advantages than ordinary heat pipes. The LHP has been applied by JPL, NASA [1]. In 1994, it occurred to David A. Wolf that the LHP, integrating the merits of the traditional pipe and capillary pump loop, would not have the restraints imposed on the traditional and capillary pump loop [2]. In 2002 NASA cooperated with the University of Cincinnati in developing a micro loop heat pipe (MLHP) by adopting micro electro mechanical systems (MEMS) technology. They analyzed the corresponding changes between the heating power and MLHP saturation temperature by simulating every condition in which various radiation temperatures were changed under a steady state [3].

This study produced a MLHP using existing MEMS technology to test its performance, and observed the relevant phenomena of the modified loop structure so that the overall system would be more applicable to microstructures and meets current heat dissipation requirements.

*Corresponding author. E-mail: swkang@mail.tku.edu.tw

2. Design, Fabrication and Packing of MLHP

2.1 Design of MLHP

This research was contacted to design a flat-plane device, so that the cooling system can be set up far away the heat source, and the heat source area can be simplified. After that we estimate the miniaturization of the device and describe the concept of design.

2.1.1 Design Guideline

MLHP consist of the evaporator, vapor line, condenser, liquid line, compensation chamber and capillary micro channels, show in Figure 1. The vapor was produced at the evaporator, and reach to the condenser along the vapor line. Then the vapor was cool down at the condenser, and the liquid return to compensation chamber by liquid line. The compensation chamber is design to re-

cruit fluid to the evaporator to avoid the dry out.

1. Heat dissipation of LHP is based on the phase change, which deprives tremendous latent heat. The performance of MLHP must be less than that of a LHP with larger diameter. Thus, designing sufficient capacity from such a small-sized space to facilitate work fluid efficiency is a major consideration.
2. The heat flow path between both the evaporator and the condenser should be thermally insulated because the evaporator is very close to the condenser where heat fails to be exchanged.
3. Because the whole system of the MLHP is fabricated on the same silicon wafer, it is mandatory to note if vapor from the evaporator reverses into the compensation chamber.
4. The width of the micro channel will influence the capillary pressure deficit of the entire system because micro fluid channels are used for pumping liquid; hence, a comprehensive design of the capillary micro channel should be provided.
5. Some experimental results of the large-sized LHP concluded that the influence of non-condensable vapor on the LHP is less significant than expected. However, non-condensable vapor actually blocks the channels because of the pipe's extremely small diameter. This point of view highlights the remarkable effects on the circulating work fluid block.

2.1.2 MLHP Design

As demonstrated in Figure 2, the convex corners of silicon micro channels subject to KOH silicon anisotropic wet etching erode, under the situation that the convex corner compensation technique is not provided on purpose herein. That is because a shrinkage cavity occurs from a larger pipe to a smaller pipe, resulting in restraining secondary head loss for the liquid flow. For example, the coefficient of head loss at a right angle is 0.78. Convex corner etching yielded from this study approximates 45° while the coefficient of head loss is 0.17 [4], is obtained from the formula table. Sparing the convex corner compensation might cause less vapor pressure deficit and maintain the system performance at a certain level of good working.

2.2 Micro-fabrication of MLHP

Figure 3 shows the fabrication process of MLHP. Silicon wafers and transparent 7740 glasses were applied as the device substrates in this study. The MLHP thickness equals to 825 μm, and the overall system for favorable theoretical analysis and optimum design could be observed accordingly. A {100} silicon wafer was used to fabricate V-groove capillary micro-channels as well as the evaporator, vapor channel, fluid channel, condenser and compensation chamber monolithically. Double-side etching was used to etch the wafer. The depth of the internal chamber reached 263 μm. The wafer and glass were hermetically bonded together using anode bonding tech-

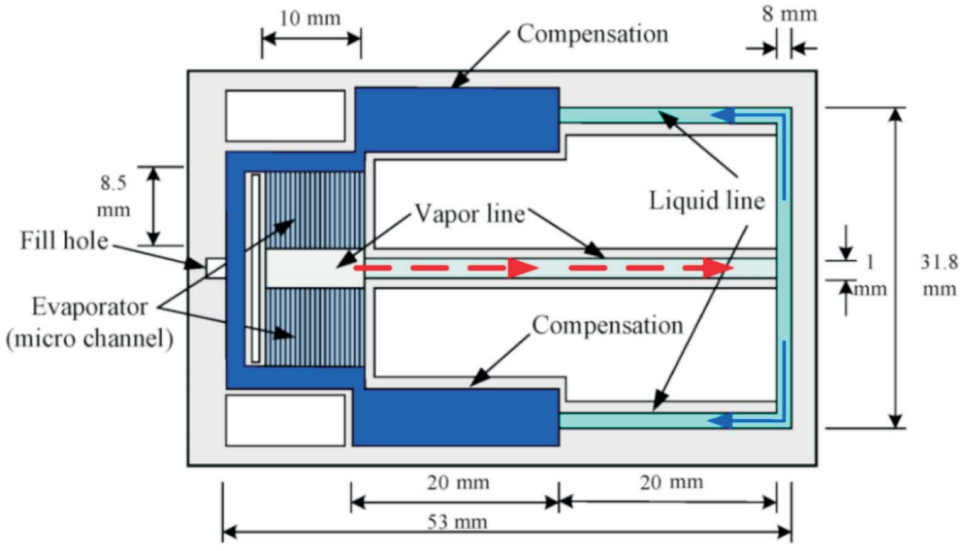

Figure 1. Layout and size dimension of MLHP.

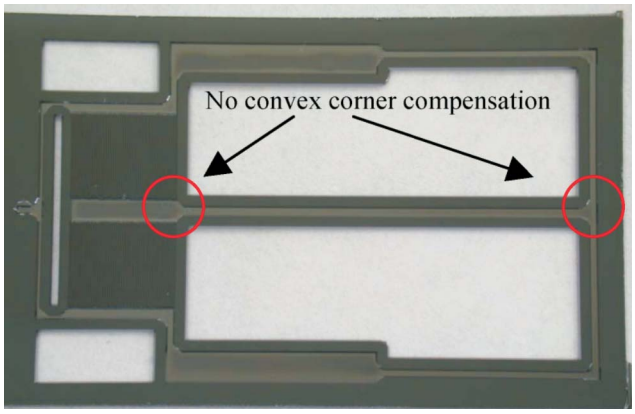

Figure 2. The MLHP chip with the size of 60 mm × 33 mm, after the anisotropic etching (KOH) process.

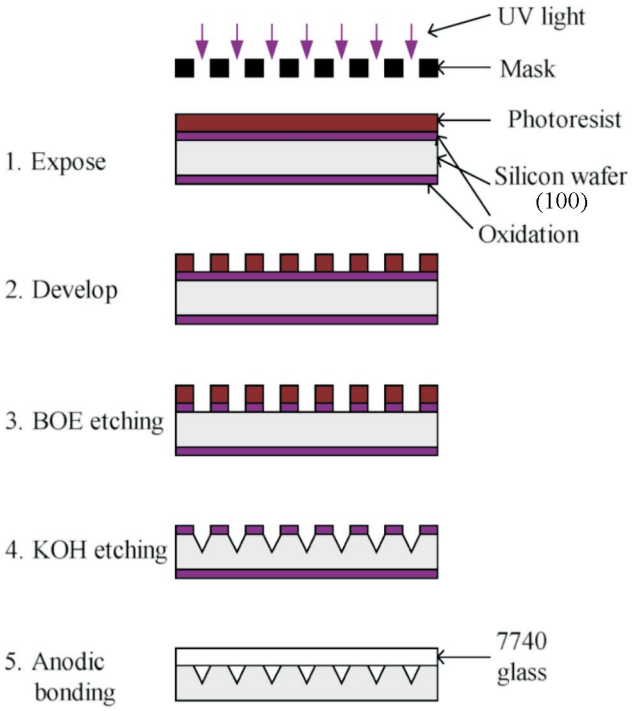

Figure 3. Process flow of micromachings for MLHP.

Figure 4. The MLHP after MEMS process and vacuum packing.

nique.

2.3 Gas Separation, Filling Work Fluid and Packaging of MLHP

How non-condensable vapor is exhausted from the MLHP and how the pipe filled with the required working fluid is explained in this section. The interior must remain in vacuum before the filling of the working fluid. The MLHP is sealed as shown in Figure 4.

Non-condensable vapor has a significant influence on the fluid circulation in the micro channels. The non-condensable vapor must be exhausted out of the MLHP chamber. The MLHP is filled with working fluid using the vacuuming approach and heating method. First, we draw out the air from the device with the 3-way valve and inject the working fluid, then by using the hot plate to heat the working fluid, we can eliminate the non-condensable vapor from the fluid.

2.3.1 Filling Volume of Work Fluid

After the working fluid is heated in the MLHP, some of the fluid is converted into vapor. There will then be a vapor fluid distribution in the MLHP. According to Maidanik [5], there is a formula for filling the LHP volume:

$$V_{wf} = \varepsilon V_w + V_{ll} + V_{cc} + V_{cch} \tag{1}$$

The work fluid fill volume V_{wf} shall be equal to the total volume of the vacant capillary structure εV_w, fluid channel V_{ll}, compensation chamber V_{cc} and the compensation chamber core V_{cch}. The parameter refers to the capillary structure porosity. The formula in this study with the compensation chamber core refers to the MLHP fill volume as:

$$V_{wf} = \varepsilon V_w + V_{ll} + V_{cc} \tag{2}$$

The work fluid accounts for 60% to 80% of the MLHP capacity. Various fill volumes will affect the saturation pressure in the MLHP. The chief consideration is based on the adequate fluid supply for the evaporator capillary structure. It is therefore not the filling volume but the capillarity that has a crucial influence on the MLHP heat-conducting performance. So we utilize the immobile filling volume to test the MLHP heat-con-

ducting performance.

3. Experimental Measurements and Flow Visualization of MLHP

3.1 Performance Assessment

Because heat dissipation comes from the tremendous latent heat deprived by the phase change, the thermal conductivity depends on how much heat flux can be deprived by the heat dissipation device from the heat source.

MLHP consists of several components. It is not formed as simple as a conventional heat pipe. With the performance analysis directly indicated by thermal conductivity coefficient k, temperature difference T and thermal resistance, channel geometry L and A, the MLHP heat dissipation efficiency is analyzed by evaluating the thermal resistance R. The thermal resistance formula is shown as below:

$$Q = \frac{AK}{L}\Delta T = \frac{\Delta T}{R} \tag{3}$$

$$R = \frac{L}{AK} = \frac{\Delta T}{Q}(^{\circ}\mathrm{C/W}) \tag{4}$$

ΔT indicates the temperature difference between the evaporator exit and the condenser entrance.

3.2 Experiment Set-up

The temperature changes in the MLHP were measured at every power level to evaluate the performance of the MLHP. Flow visualization was used to verify the feasibility of the fabricated device of the MLHP. Figure 5 shows the set-up of the test platform.

This system is a heat exchange mechanism. The input heat source and cooling system are indispensable. Thermocouple wires were used to acquire the temperatures of the assigned positions shown in Figure 6, so that the heat dissipation efficiency could be calculated.

A ceramic heater was used as the heat source. The back of this heater was covered with insulating cork to prevent heat loss. Thermal paste was applied between the

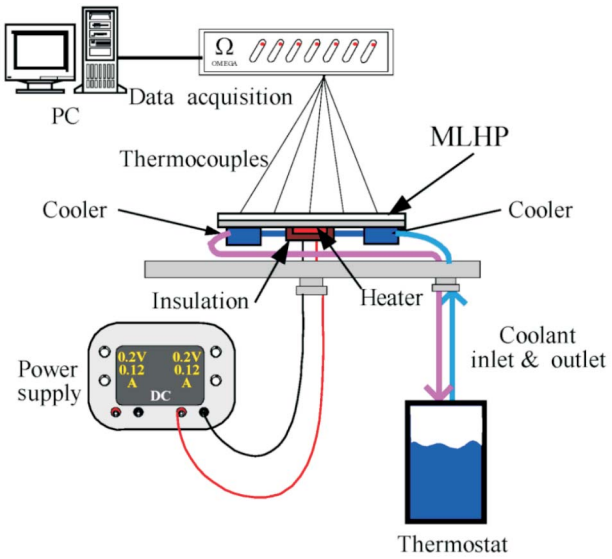

Figure 5. Test platform diagram.

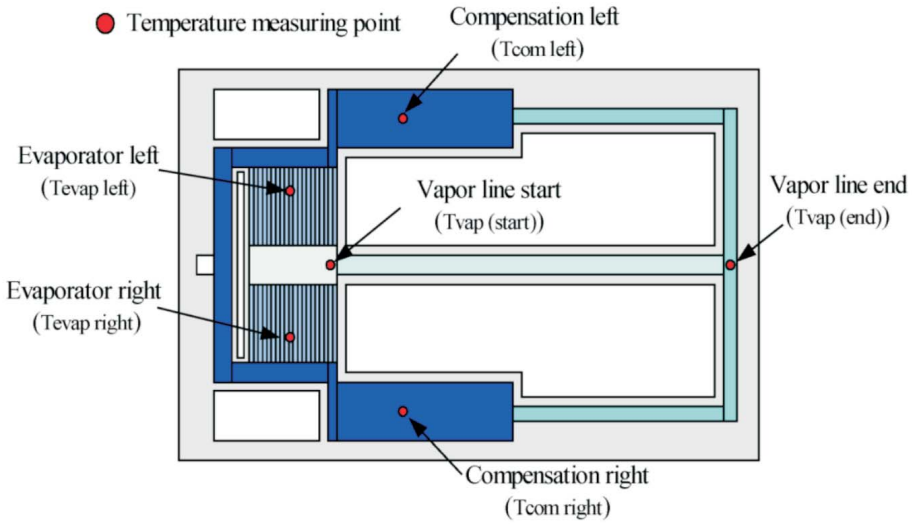

Figure 6. Position for the thermal couples using in MLHP.

ceramic heater and the MLHP to prevent the air gap at the interface from developing severe contact thermal resistance.

Two copper hexagonal joints connected with cooling pipes were used as the cooling condenser. Deionized water, 17 °C was circulated as the pipe coolant. To restrain the contact resistance, the cooler and the condenser were coated with thermal paste. The vapor and fluid channels at the interval were deemed as thermal insulators for their fast transmission and small change in temperature. No additional devices were added except cotton insulation coating the silicon pipe to prevent environmental influence.

3.3 Performance Test of MLHP

Four samples of MLHP were tested in this study. Diverse capillary structures and different work fluids were selected in this performance test, as shown in Table 1. The temperature of every point and the thermal resistance between the evaporator and condenser (referring to the 40 mm long interval between both ends of the vapor, fluid channel) were measured in this test.

The testing parameters are detailed in Table 2. To adjust the power supplier to a required level within a short lapse of time, the voltage was elevated from 6.0 V by 1.0 V per unit time. The measurement time was 180 seconds and the temperature was acquired every second. Because the ceramic heater was thin and affixed directly to the MLHP, the heat transmission was quite rapid. The steady state is verified by the real observation that the measured temperature could reach a fixed value within 60 seconds under fixed power. The temperature data for every point in the following steady state diagrams was analyzed by equalizing the second half of the forgoing 180 seconds and acquiring the steady value for each single point at every power level.

4. Experimental Analysis, Results and Discussion of MLHP

4.1 Start-up of MLHP

From Figure 7, the transient diagram, the temperature T_{vap} shows a clear decline in the first 30 seconds, when the capillary channel has a hydraulic diameter (D_h)

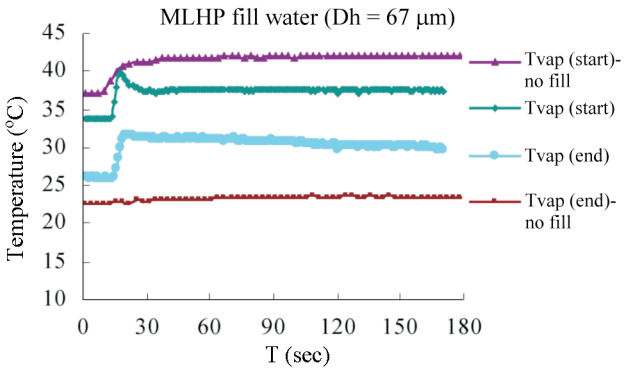

Figure 7. Transient diagram of temperature-time.

Table 1. The different of capillary structures and work fluids used in the MLHP experiment

Test Sample #	1	2	3	4
Evaporator Width of Capillary Channel (μm)	160	90	130	90
Hydraulic Diameter (D_h) (μm)	83	47	67	47
Number of Micro Channels	33	83	42	83
Work Fluid	D. I. water	D. I. water	Methanol	Methanol

Table 2. The testing parameters of the MLHP experiment

Test Sample #	1	2	3	4
Work Fluid	D. I. Water	D. I. Water	Methanol	Methanol
Sized of Capillary Micro Channel (D_h) (μm)	83	47	67	47
Thermal Power Range Voltage Controlled (V)	6.0 – 19.0	6.0 – 21.0	6.0 – 20.0	6.0 – 19.0
Corresponding Heating Power Range (W)	1.14 – 12.92	1.14 – 15.96	1.20 – 14.80	1.20 – 13.11
Voltage Added per Time (V)	1.0	1.0	1.0	1.0
Measurement Time for per Voltage (sec)	180	180	180	180
Total Experiment Measurement Time (min)	42	48	45	42

of 67 μm and the working fluid is deionized water. The healthy power increased from 2.7 W to 3.3 W, and reached a steady state in approximately 10 seconds. This means that the MLHP has started. If we follow the previous rule with no filling, a higher temperature will occur. But, as working fluid enters and moves, sub-cooling fluid in the compensation chamber will be supplied to the capillary structure in the evaporator. This will lower the temperature and meet the mission of MLHP basically. When the MLHP is filled with working fluid, the temperature difference between the front end and back end of the vapor/fluid channel is less than the temperature difference of the case that the non-filled MLHP because vapor flow works and moves in the interior.

4.2 Influences from MLHP's Degree of Sub-cooling

Due to the deficient sub-cooling and ineffective capillary structure thermal insulation (thermal conductivity coefficient of silicon is as high as 150W/mK), thermal leakage always leads to higher temperatures in the test platform compensation chamber and make the condensed reversed fluid vaporized. Under these circumstances, the evaporator cannot be supplied with working fluid backflow. The vapor then fails to reverse into the fluid channels and flows back to the vapor channels or even the evaporator region again. Finally the working fluid in the evaporator is dried out and the cooling mechanism is stopped.

The test approach was changed based on this consideration. The condenser was placed under two compensation chambers to provide a chamber for storing work fluid, condensing and vaporizing. Hence, the degree of sub-cooling in the compensation chamber could be used to keep the working fluid in the liquid state. A temperature contrast between non-filled working fluid and the MLHP (as in Figure 8) was made under various experimental conditions.

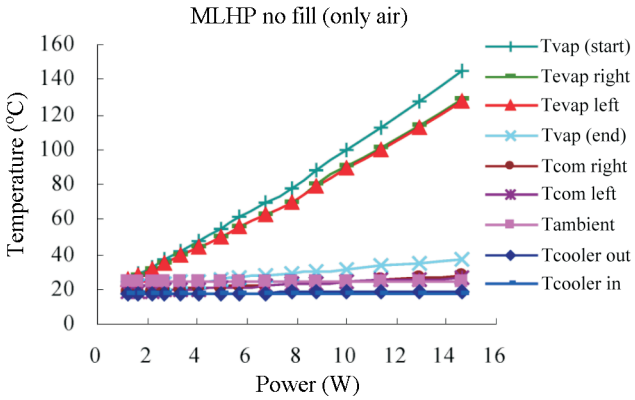

Figure 8. Steady state diagram on MLHP test platform (no work fluid filled).

4.3 MLHP Performance Analysis between Different Capillary Structure

Capillary micro channels with different hydraulic diameters will produce a discrepancy in the overall performance of heat transmission. However, the fill volume of working fluid does not affect the MLHP performance because the mechanism operation in not influenced if the evaporator has an unfailing supply of sub-cooling fluid from the compensation chamber. The number of capillary micro channels has the greatest influence the performance.

The MLHP performance analysis of the four test samples of MLHP herein are discussed in the followings, respectively:

Test Sample #1 D_h of the Capillary Micro Channel: 83 μm, Work Fluid: D. I. Water

From Figure 9, when the power is increased to 3.3 W, the evaporator temperature and the front vapor channel temperature also increase. The MLHP begins to operate. At 4 W, the back end vapor channel temperature begins to increase acutely. This indicates that the vapor flow has reached the back end, reducing the temperature differ-

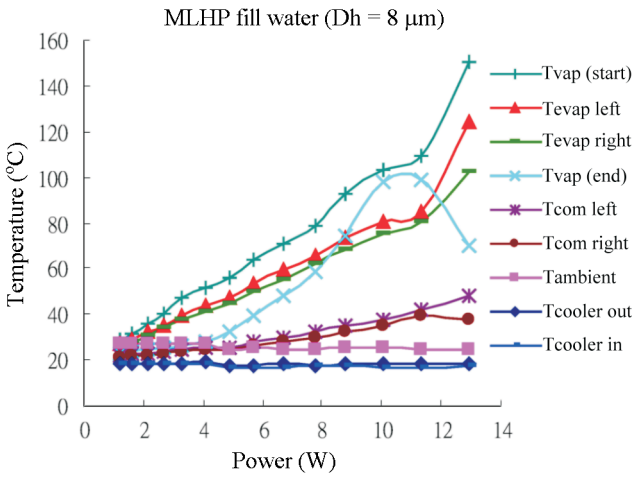

Figure 9. Steady state diagram of temperature and power (D_h of the micro channel = 83 μm, filled with D. I. water, test sample #1).

ence between both ends. Accordingly, the thermal resistance of both ends is decreasing while the thermal conductivity performance is increasing. The thermal resistance reaches the minimum when the power is set between 10.03 W and 11.34 W while the T_{evap} is kept between 74 °C and 80 °C.

When the power exceeds 11.34W, a dry burn is developed to increase the temperature sharply in case the backflow from the capillary structure fails to supply the evaporator with vaporized fluid under high power (watt). At the same time excessive thermal leakage reverses the steam into the compensation chamber. As the fluid in the micro channel is dried out, which generates steam between the capillary structure and the compensation chamber, the sub-cooling fluid is pushed back into the steam channel to fill the back end of the vapor channel with fluid. The temperature then decreases sharply.

When the power increases to 3.3 W the system achieved with optimal thermal conductivity is obtained at 10.03 W – 11.34 W. Once the power exceeds 11.34 W, the MLHP process gets lost with its function.

Test Sample #2 D_h of the Capillary Micro Channel: 47 μm, Work Fluid: D. I. Water

From Figure 10: when the power increases to 3.3 W, the evaporator and front-end temperature of the vapor channel also rise slowly. Simultaneously, the MLHP begins to operate. However, when the power is at 4W, the back end vapor channel temperature begins to increase sharply. Although the MLHP mechanism operates indistinctly, it indicates that the vapor flow has reached the back end and the thermal resistance of both ends is decreasing. The thermal resistance reaches the lowest when the power lies between 7.8 W and 12.92 W and the evaporator temperature does not exceed 80 °C.

A dry burn is developed when the power exceeds 12.92 W that sharply raises the temperature. The back end of the vapor channel is then filled with reversed fluid, sharply decreasing the temperature.

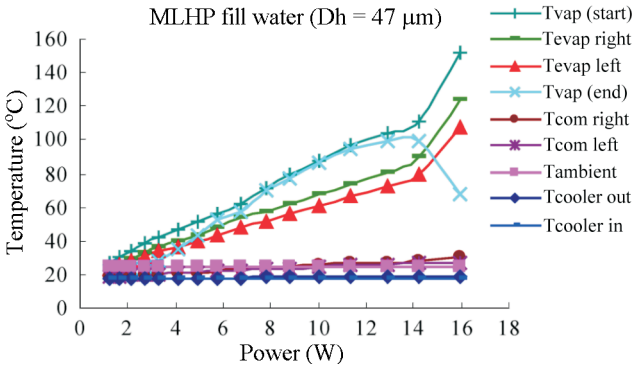

Figure 10. Steady state diagram of temperature and power (D_h of the micro channel = 47 μm, filled with D. I. water, test sample #2).

Test Sample #3 D_h of the Capillary Micro Channel: 67 μm, Working Fluid: Methanol

From Figure 11: Methanol begins to operate at 1.20 W, while the back end vapor channel temperature rises swiftly. The temperature difference between both ends of the vapor channel is the least when the power lies between 2.16 W and 3.40 W. However, the evaporator temperature rise suddenly when the power exceeds 3.4 W, while the back end vapor channel temperature declines acutely. Through flow visualization, the evaporator cap-

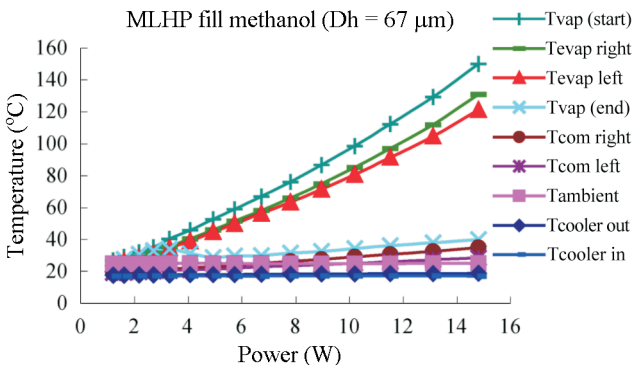

Figure 11. Steady state diagram of temperature and power (D_h of the micro channel = 67 μm, filled with methanol, test sample #3).

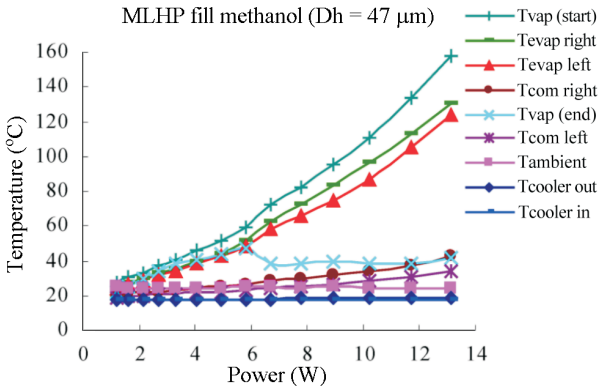

Figure 12. Steady state diagram of temperature and power (D_h of the micro channel = 47 μm, filled with methanol, test sample #4).

illary structure is completely dried out and the entire MLHP is ineffective when the power exceeds 3.4W. This differs greatly from a MLHP filled with D. I. water.

Test Sample #4 D_h of the Capillary Micro Channel: 47 μm, Work Fluid: Methanol

Figure 12 is similar to Figure 11 in which methanol begins operating at 1.20 W. The temperature difference between both ends of the vapor channel is the least when the power lies between 2.16 W and 5.85 W. The evaporator temperature rises suddenly when the power exceeds 5.85W, while the back end vapor channel temperature declines acutely. Through flow visualization, the entire MLHP is nearly ineffective when the power exceeds 5.85W.

4.4 MLHP Temperature and Thermal Resistance Performance Contrast under Various Evaporator Terms

A contrast experiment was conducted between the evaporator temperatures on top of the heat source and a relative analysis of the thermal resistance at non-filling and the thermal resistance corresponding to other terms.

4.4.1 Temperature Contrast under Various Evaporator Terms

The right and left sides of the MLHP can be regarded as two respective systems. If one side has no function, the other side can even operate. Thus, a difference in temperature between both sides of the evaporator could occur. The temperatures of both evaporator sides were equalized for a contrast between the average temperature and the temperature when the MLHP is not filled with working fluid (as shown in Figure 13). From Figure 13, we find that the evaporator temperature differs from the temperature at non-filling, when water is used as the working fluid.

The analysis was implemented under 90 °C and the contrast was conducted only when the operating mechanism was still effective.

Test sample #1, the largest difference between the present temperature filled with D. I. water and non-filled evaporator temperature occurred at a heat power of 10.03W. The evaporator temperature of the non-filled MLHP was 90 °C while the temperature difference was 12.3 °C, i.e. a present temperature of 77.7 °C.

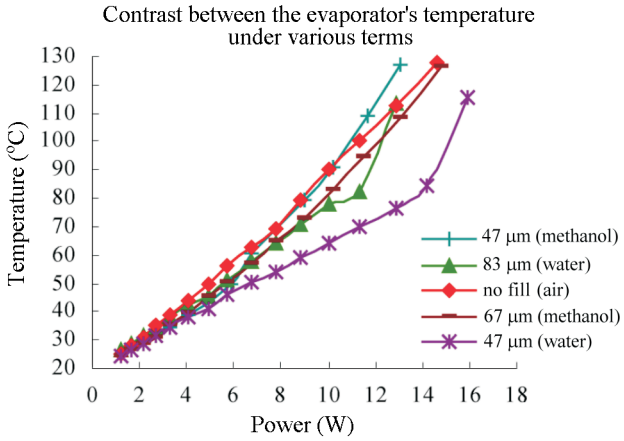

Figure 13. Contrast between the evaporator's temperature under various terms of MLHP.

Test sample #2, the largest difference between the present temperature and non-filled evaporator temperature occurred at a heat power of 10.03 W. The evaporator temperature of the non-filled MLHP was 90 °C while the temperature difference was 26 °C, i.e. a present temperature is 64 °C.

Test sample #3, the system worked and the largest difference between the present temperature and non-filled evaporator temperature occurred at a heat power of 3.3 W. The evaporator temperature of the non-filled MLHP was 39.2 °C while the temperature difference was 4 °C, i.e. a present temperature is 35.2 °C.

Test sample #4, methanol was used the system still worked and the largest difference between the present temperature and non-filled evaporator temperature occurred at a heat power of 5.85 W. The evaporator temperature of the non-filled MLHP was 56 °C while the temperature difference was 6 °C, i.e. a present temperature is 50 °C.

From the preceding discussion or observation, we conclude that filling with water leads to a stronger drop in the evaporator temperature, and features better performance than methanol. We also discovered that water is favorable to the operation of the entire system at larger power (watt) while methanol's best performance occurred at lower power.

4.4.2 Thermal Resistance Contrast under Various Terms

The best MLHP performance occurred when the cooling mechanism was working, that is, in the opera-

tion temperature and tolerable heating power range. Thus, the thermal resistance does not correlate power distribution with a linear behavior. This experiment focused on the thermal resistance of the interval between both vapor channel ends where steam is vaporized by the evaporator and flows in. This part of the operation is equal to the work fluid in the conventional heat pipe, heated by the evaporator and generating steam flowing to the condenser. However, in the conventional heat pipe the vapor, fluid channel produces an "entrainment limit" and results in lower performance. Based on this, we designed the vapor channel and fluid channel separately for the MLHP to enhance the thermal conductivity efficiency.

From Figure 14, the thermal resistance between both the vapor channel ends (with a distance of 40 mm) ranged from 4 °C/W to 7 °C/W when no work fluid filled the MLHP. After filling with methanol, the interior mechanism began working with the MLHP thermal resistance dropping to 2 °C/W. As mentioned before, the MLHP cannot begin operating under all conditions. This is because the MLHP is subject to capillarity action and the working fluid operating temperature. The thermal resistance provides better performance only in specific power ranges. In Figure 14, a lower thermal resistance was acquired where D_h = 67 μm and the power range was between 1.61 W and 4.07 W. The optimum thermal resistance of 0.568 °C/W occurred at 2.16 W power. When D_h = 47 μm, the power range was 2.16 W to 5.85 W. The optimum thermal resistance of 0.787 °C/W occurred at 3.4 W power.

When water was used as the working fluid, as observed in Figure 15, the thermal resistance performance was better than Methanol. We acquired a lower thermal resistance when D_h = 83 μm and the power range was between 8.8 W and 11.34 W. The optimum thermal resistance of 0.575 °C/W occurred at 10.03 W power. The thermal resistance was lower when D_h = 47 μm and the power range was between 4.8 and 14.2 W. The optimum thermal resistance of 0.106 °C/W occurred at 10.03 W power.

From the forgoing discussion, the thermal resistance is retained at a smaller value at larger power when the capillary structure size is smaller. Deionized water as the working fluid features more favorable performance than methanol. The optimum thermal resistance occurred when

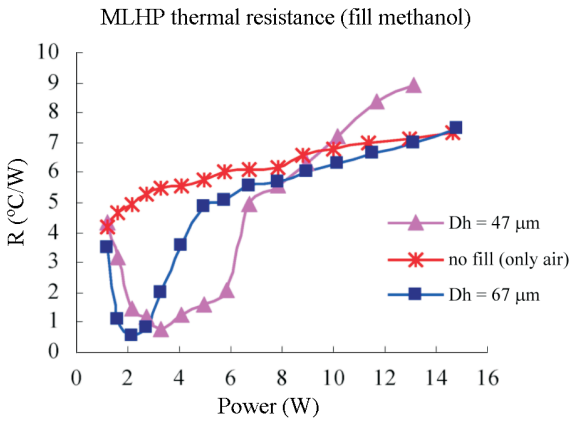

Figure 14. Steady state diagram of thermal resistance and heating power.

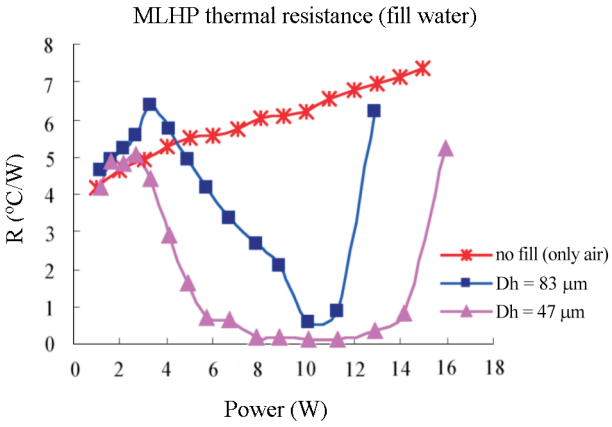

Figure 15. Steady state diagram of thermal resistance and heating power (filled with D.I water).

D. I. water was used and D_h = 47 μm. The MLHP operating power range is also wider than that with methanol. Although methanol can begin operating at lower power, D. I. water provides better overall operating efficiency. The fluid density and latent heat is less than those of D. I. water, as a result, the lower heat capacity of methanol fails to supply the high thermal conductivity required at high power.

5. Conclusion

This paper discussed the miniaturization and the performance testing for MLHP. The biggest challenge is how to design the MLHP structure and shape of MLHP. The capillary structure of the MLHP was designed using micro channels made of silicon. This micro channel features good thermal conductivity and produces excessive

heat leakage in the compensation chamber. A cooler was placed under the compensation chamber for cooling and the vapor channel and fluid channels were connected directly. Therefore, the fluid in the compensation chamber could be retained at a specific degree of cooling to facilitate entire system operation. Some observations were summarized as below:

(1) Influence from non-condensable vapor: In this study, we proved that non-condensable vapor has a significant influence on a miniaturized LHP and overloads the MLHP with excessive pressure resulting in a fragmented test wafer.

(2) Influence from different work fluids: We use D. I. water and methanol as the working fluid in this study. Because D. I. water enhances the MLHP power to 11.3 W (where D_h of the capillary micro channel = 83 μm) and maintains the operating mechanism until 12.92 W. D. I. water was therefore superior to methanol as a working fluid. Water also allows a higher operating power than methanol.

(3) Influence from capillary structure: The results of this experiment verified that a smaller sized capillary structure is more beneficial for MLHP operation. It also allows a broader power range for MLHP operation than the larger sized structure. Moreover, the MLHP is fabricated on the same plane. Two capillary structure rows are inadequate. Increasing the number of capillary structure rows is an important issue because its performance is based on the diameter and quantity of micro channels.

(4) Start-up temperature of MLHP: Methanol begins operating at 24.69 °C and transmits steam from the evaporator to the condenser. D. I. water begins its operation at 31.64 °C.

(5) Performance assessment of MLHP: Compared with methanol, D. I. water produces a sharper drop in temperature, up to 26 °C. From the performance analysis, the thermal resistance of D. I. water is lower than that of methanol. The optimum thermal resistance of the MLHP using D. I. water is 0.106 °C/W, which is 64 times larger than the thermal resistance of the MLHP without working fluid. This proves that the thermal conductivity performance of water is better than the solid thermal conductivity mechanism.

Acknowledgment

This work was supported by the National Science Council of Taiwan, Republic of China under contract No. NSC 92-2212-E-032-002.

References

[1] NASA Jet Propulsion Laboratory, www.jpl.nasa.gov.

[2] Wolf, D. A., et al., "Loop Heat Pipe-Their Performance and Potential," *Dynatherm Corporation Inc, SAE Technical Paper* No. 941575 (1994).

[3] Kim, J. and Golliher, E., "Steady State Model of a Micro Loop Heat Pipe," *18th IEEE SEMI-THERM Symposium*, pp. 137–144 (2002).

[4] Fox, R. W. and Mcdonald, A. T., *Introduction to Fluid Mechanics Fifth_Edition*, Wiley, NY, U.S.A. pp. 363–364 (1998).

[5] Maidanik, Y. F., "Loop Heat Pipes Technology," *Solar Energy and Technology Conference*, Taipei, Taiwan, pp. 50–56 (2000).

Manuscript Received: Jan. 3, 2005
Revision Received: Jan. 14, 2005
Accepted: Mar. 15, 2005